# Biosynthesis of Chlorophyll *a* in a Purple Bacterial Phototroph and Assembly into a Plant Chlorophyll−Protein Complex

Andrew Hitchcock,[†] Philip J. Jackson,[†,‡] Jack W. Chidgey,[†] Mark J. Dickman,[‡] C. Neil Hunter,*,[†] and Daniel P. Canniffe[†,§]

[†]Department of Molecular Biology and Biotechnology, University of Sheffield, Sheffield S10 2TN, U.K.
[‡]ChELSI Institute, Department of Chemical and Biological Engineering, University of Sheffield, Sheffield S1 3JD, U.K.

S *Supporting Information*

ABSTRACT: Improvements to photosynthetic efficiency could be achieved by manipulating pigment biosynthetic pathways of photosynthetic organisms in order to increase the spectral coverage for light absorption. The development of organisms that can produce both bacteriochlorophylls and chlorophylls is one way to achieve this aim, and accordingly we have engineered the bacteriochlorophyll-utilizing anoxygenic phototroph *Rhodobacter sphaeroides* to make chlorophyll *a*. Bacteriochlorophyll and chlorophyll share a common biosynthetic pathway up to the precursor chlorophyllide. Deletion of genes responsible for the bacteriochlorophyll-specific modifications of chlorophyllide and replacement of the native bacteriochlorophyll synthase with a cyanobacterial chlorophyll synthase resulted in the production of chlorophyll *a*. This pigment could be assembled *in vivo* into the plant water-soluble chlorophyll protein, heterologously produced in *Rhodobacter sphaeroides*, which represents a proof-of-principle for the engineering of novel antenna complexes that enhance the spectral range of photosynthesis.

KEYWORDS: photosynthesis, chlorophyll, bacteriochlorophyll, antenna complex, water-soluble chlorophyll protein, *Rhodobacter sphaeroides*
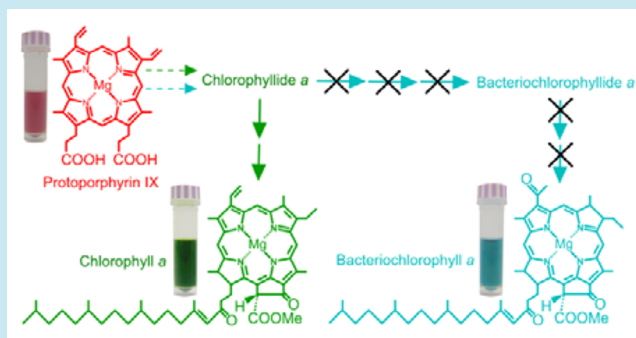
The overall efficiency of photosynthesis, measured on the basis of conversion to biomass, is in the region of 1−7%.[1] The primary steps of solar energy harvesting and charge separation, although inherently extremely efficient, are still constrained by the small portions of the available solar spectrum that can be absorbed by the light-harvesting pigment−protein complexes, which have evolved to be sufficient for survival in their particular ecological niche. One approach hypothesized to improve the efficiency of energy capture is to broaden the range of wavelengths absorbed by a biological system by producing mixtures of pigments, or mixtures of photosystems, in the same cell.[1,2] In oxygenic phototrophs, where the two photosystems are in competition for the same wavelengths of light, it has been proposed that re-engineering PSII and PSI to absorb light from different regions of the solar spectrum could improve energy capture, with potential positive impacts on growth rates and therefore crop yields and season lengths.[3]

The major photon absorbing pigments involved in solar energy capture are the (bacterio)chlorophylls ((B)Chls), housed in the antenna complexes of plants, algae and phototrophic (cyano)bacteria. The spectral range of these complexes is altered by modifications to the (B)Chl macrocycle, which shifts the red-most absorption band from ∼680 nm in the case of Chl *a*, to 800−920 nm for BChl *a* and as far

as 1023 nm in the case of antennas containing BChl *b*. These pigments share a common pathway up to the biosynthetic intermediate chlorophyllide (Chlide), the direct precursor of Chl *a* (Figure 1a). In the case of the true BChls, Chlide is converted to a bacteriochlorophyllide species (BChlide) by further modifications to rings A and B, extending the Q_y absorption bands of BChl pigments into the near-infrared[4] and allowing anoxygenic phototrophic bacteria to harvest light that is not absorbed by the oxygenic algae and cyanobacteria higher in the water column/microbial mat.[5]

In the purple phototrophic bacterium *Rhodobacter* (*Rba.*) *sphaeroides*, the major BChl absorption bands are in the 375−400, 580−600 and 800−900 nm spectral regions, with carotenoids providing additional absorption between 400 and 550 nm. Thus, there is a spectral region between 600 and 800 nm with no major absorption features that could be occupied by a pigment such as Chl *a*. BChl *a* pigments within the peripheral (LH2) and core (LH1) antenna effectively funnel absorbed solar energy to the photosynthetic reaction center (RC), where charge separation occurs.[6,7] In order to establish a photosystem capable of harvesting a wider range of wave-
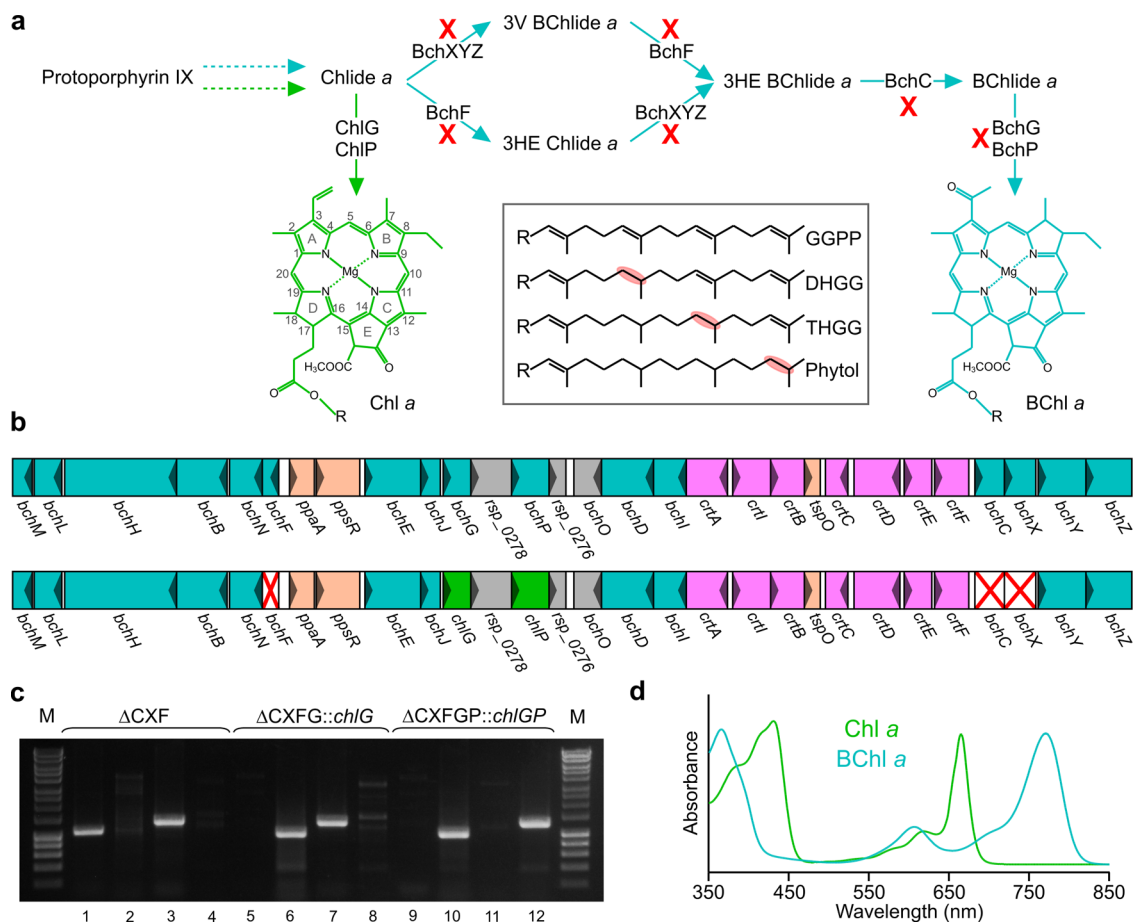
Figure 1. Concept for constructing a Chl *a* biosynthesis pathway in the purple phototroph *Rba. sphaeroides*. (a) The native BChl *a* biosynthetic pathway (blue arrows). Removal of BchF, BchX and BchC (red cross) from the native pathway halts the production of BChl at the level of Chlide, and ChlG and ChlP from *Synechocystis* (green arrows) are introduced to reroute the pathway to Chl *a*. Dashed arrows represent multiple enzymatic steps. Chemical structures of Chl *a* (IUPAC numbered) and BChl *a* are shown. 3V, C3-vinyl; 3HE, C3-hydroxyethyl. R denotes the attached alcohol moiety. Inset: Alcohol moieties of (B)Chls, denoted by R. Highlighted bonds are those sequentially reduced by the gene product of *chlP/ bchP*. GGPP, geranylgeranyl pyrophosphate; DHGG, dihydrogeranylgeranyl pyrophosphate; THGG, tetrahydrogeranylgeranyl pyrophosphate. (b) The organization of native (upper) and modified (lower) partial photosynthesis gene clusters of *Rba. sphaeroides*. Blue, *bch* genes; magenta, *crt* genes; peach, regulatory genes; gray, unassigned genes. Deletions of *bchF*, *C* and *X* (red cross) in the native pathway are shown as well as the sites where the native *bchG* and *bchP* were replaced by *chlG* and *chlP* from *Synechocystis* (green). (c) Agarose gel of PCR products confirming the replacement of *bchG* with *chlG* in ΔCXFG::*chlG* and *bchG* and *bchP* with *chlG* and *chlP* in ΔCXFGP::*chlGP*. In each PCR reaction a *bchG/P* or *chlG/P* specific forward primer was used with a reverse primer in the downstream rsp_0278 (for *bchG/chlG*) or rsp_0276 (for *bchP/chlP*) gene. Lanes 1, 5, 9 = *bchG* specific primers; lanes 2, 6, 10 = *chlG* specific primers; lanes 3, 7, 11 = *bchP* specific primers; lanes 4, 8, 12 = *chlP* specific primers; M = Hyperladder 1kb (Bioline). (d) Absorption spectra of methanol extracted (B)Chl pigments.

lengths, it will ultimately be necessary to engineer an organism capable of making a mixture of Chl and BChl pigments. BChl biosynthesis can be viewed as an extension of the Chl pathway, so the production of Chl *a* in a photosynthetic bacterium can be achieved by truncation of native BChl biosynthesis, along with modifications to introduce Chl-specific enzymes that attach and reduce the isoprenoid alcohol moiety (Figure 1a), which decisively increases the hydrophobicity of the pigment. Here we report the implementation of this strategy using *Rba. sphaeroides* as a chassis; this anoxygenic phototroph has a versatile metabolism permitting viability under oxic conditions in the dark, allowing for the deletion, replacement and addition of genes involved in pigment biosynthesis and photosynthesis.[8,9] The introduction of cyanobacterial Chl-specific enzymes into a Chlide-accumulating mutant of *Rba. sphaeroides* resulted in successful rerouting of BChl biosynthesis and the production of Chl *a*, the first time this ubiquitous oxygenic photopigment has been synthesized in a purple phototrophic

bacterium. As a proof-of-principle for incorporating this engineered pigment into a chlorophyll-protein complex we further demonstrate that this non-native pigment can be sequestered by the eukaryotic water-soluble chlorophyll protein[10] from Brussels sprout (*Brassica oleracea* var. *gemmifera*), BoWSCP, also heterologously produced in the Chl *a* accumulating strain of *Rba. sphaeroides*.

The assembly of a plant chlorophyll-protein complex in a photosynthetic bacterium represents an initial step in the design of a novel, high-energy Chl *a*-containing antenna that could be able to funnel excitation energy toward the native, lower energy, BChl *a*-containing light-harvesting antenna (LH2 and LH1) and RCs. In order to provide the Chlide substrate for the production of Chl *a* in *Rba. sphaeroides*, a mutant (ΔCXF) blocked at the steps exclusive to BChl biosynthesis (Δ*bchC*, Δ*bchX* and Δ*bchF*) was used as a host (Figure 1b).[11] This mutant accumulates Chlide, demonstrating that the BChl synthase (BchG) encoded by the native *bchG*

gene is unable to esterify this pigment to produce a Chl species, as reported *in vitro*,[12] and therefore cannot grow prototrophically. In order to attach an alcohol moiety to Chlide in this strain, the native *bchG* gene was replaced with the gene encoding the Chl synthase enzyme (ChlG) from the cyanobacterium *Synechocystis* sp. PCC 6803 (hereafter *Synechocystis*), codon-optimized for expression in *Rba. sphaeroides*, generating strain Δ*CXFG::chlG* (Figure 1b and 1c). Similarly, the native *bchP* gene encoding the geranylgeranyl reductase was also replaced with a codon-optimized version of *Synechocystis chlP*, generating strain Δ*CXFGP::chlGP* (Figure 1b and 1c). The sequences of the codon-optimized genes are given in Table S1.

The pigments that accumulated in these strains, along with those from the WT and Δ*CXF*, were extracted from pellets of microoxically grown cells and analyzed by HPLC (Figures 1d and 2). As expected, the WT accumulated BChl *a* (Figure 2a),
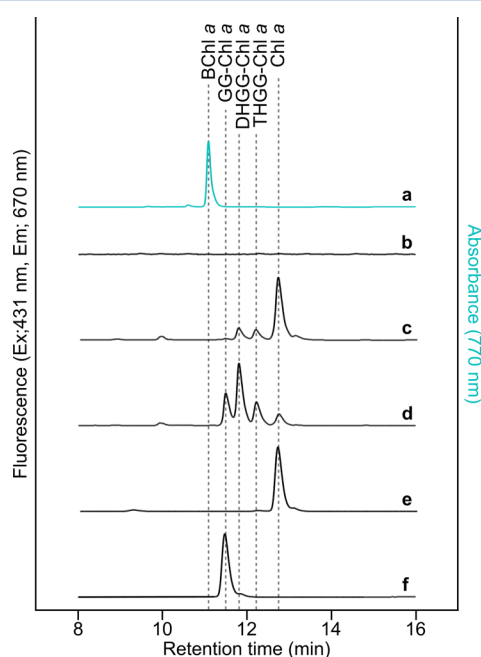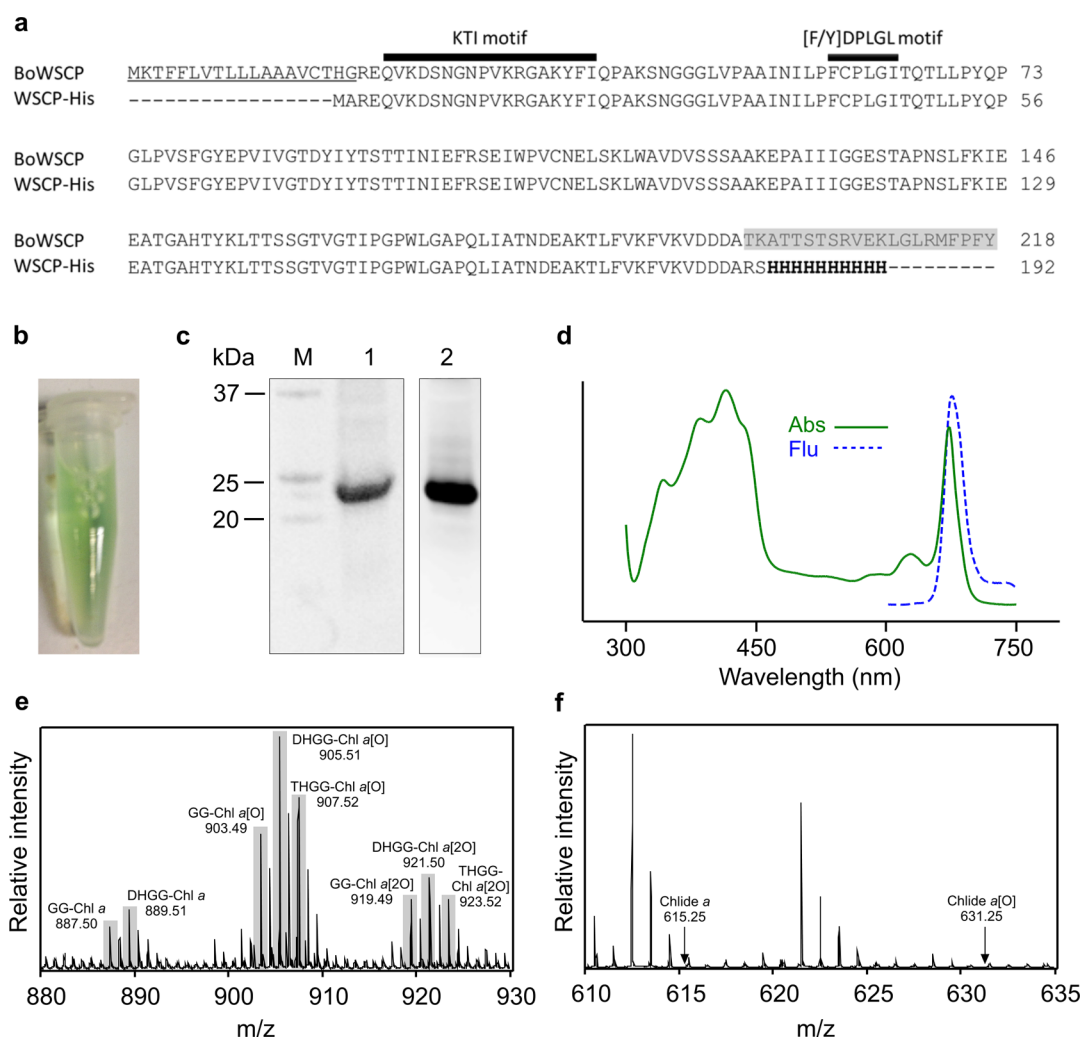

Figure 2. HPLC analysis of (B)Chls extracted from described strains of *Rba. sphaeroides*. Elution profiles of pigments extracted from pellets of (a) WT, (b) Δ*CXF*, (c) Δ*CXFG::chlG*, (d) Δ*CXFGP::chlGP*, (e) standard of Chl *a* from WT *Synechocystis*, (f) standard of GG-Chl *a* from a Δ*chlP* strain of *Synechocystis*. Elution of BChls and Chls was monitored by absorbance at 770 nm (blue) or by fluorescence emission at 670 nm with excitation at 431 nm (black), respectively. Traces are normalized to major peak height for clarity.

while Δ*CXF* was unable to synthesize (B)Chl pigments (Figure 2b). With our engineered strains, both the Δ*CXFG::chlG* and Δ*CXFGP::chlGP* strains synthesize four species of Chl *a*, esterified with geranylgeranyl-(GG), dihydroGG- (DHGG), tetrahydroGG- (THGG) or phytol moieties (Figure 1a inset panel), with each detected by fluorescence emission at 670 nm (Figure 2c and 2d). To confirm the identity of these pigments, Chls synthesized by WT and Δ*chlP* (Figure S1) strains of *Synechocystis* were used as HPLC standards for Chl *a* (Figure 2e) and GG-Chl *a* (Figure 2f) respectively. In all cases the detected pigments were confirmed to be species of BChl *a* or Chl *a* by their absorption spectrum (Figure 1d).

The most prominent pigment extracted from the Δ*CXFG::chlG* strain was Chl *a*, with only extremely low amounts of GG-Chl *a* and intermediate levels of DHGG- and THGG-Chl *a*, showing that the native BchP is able to perform three reductions of GG-Chl *a*, albeit at a lowered efficiency when contrasted with the accumulation of a single fully reduced BChl *a* species in the WT (Figure 2a). We hypothesized that this lower efficiency may be due to BchP acting on an unnatural substrate and that replacement of the native *bchP* gene with the *Synechocystis* homolog, which has previously been shown to be active in *Rba. sphaeroides*,[13] may result in more efficient tail reduction such that only Chl *a* with a fully reduced isoprenoid tail would accumulate. However, strain Δ*CXFGP::chlGP* shows no improvement over Δ*CXFG::chlG* in this respect and the proportion of fully reduced phytol-Chl *a* is actually lower than when the native BchP is used (Figure 2d). This aspect of the engineered Chl *a* pathway in *Rba. sphaeroides* requires further study of the expression and subunit composition of BchP/ChlP enzymes.

In order to sequester the engineered Chl pigments we used mature BoWSCP lacking its 19 residue amino(N)-terminal endoplasmic reticulum signal peptide[14] and post-translationally cleaved 21 residue carboxy(C)-terminal extension peptide[15] (Figure 3a); this construct was codon optimized (Table S1) and expressed with a C-terminal 10xHis-tag in the Δ*CXFGP::chlGP* strain of *Rba. sphaeroides*. Recombinant WSCP-His was purified from cell free extracts by immobilized metal affinity chromatography (IMAC) and protein fractions that contained Chl (Figure 3b), as judged by absorbance at 280 and 665 nm, were pooled, concentrated and analyzed by SDS-PAGE and immunoblotting (Figure 3c). The major Coomassie stained band corresponds to a protein of the predicted MW of WSCP-His (20.8 kDa) (Figure 3c lane 1), which cross-reacts with an anti-6-His antibody (Figure 3c lane 2). WSCP-His was identified as the predominant protein species following affinity purification by mass spectrometry analysis (Table S2, data uploaded to the ProteomeXchange Consortium[16] *via* the PRIDE partner repository, identifier 10.6019/PXD002638). The absorption spectrum of the purified pigment−protein complex (Figure 3d, solid green line) has 6 peaks (summarized in Table 1) and a small shoulder at ∼584 nm, in agreement with the spectra previously reported for native and thylakoid or Chl *a* reconstituted BoWSCP;[14,17] excitation at 431 nm resulted in fluorescence emission at ∼670 nm, as expected for Chl *a* (Figure 3d, dashed blue line). The pigment bound to WSCP-His was isolated by solid phase extraction and identified by mass spectrometry. GG-, DHGG- and THGG-Chl *a* were identified, but not Chl *a* or Chlide (Figures 3e, 3f and S2). Tight binding to the WSCP-His could account for the failure to detect Chl *a*.[10] It is interesting that Chlide was not detected, showing that WSCP-His selectively binds esterified Chl *a* over an excess of the less hydrophobic precursor, which accumulates in this strain.[11]

The production of Chl *a* does not restore photoautotrophic growth to the Δ*CXF* mutant as *Rba. sphaeroides* cannot use this pigment for light harvesting or photochemistry. Furthermore, only a small amount of Chl *a* is produced compared to BChl *a* in the wildtype organism (approximately 0.1%), which is not surprising as a mutant of *Rba. sphaeroides* harboring deletions in genes encoding photosystem apoproteins accumulates no BChl despite having an intact pigment biosynthesis pathway.[18] This observation shows that, in the absence of the appropriate binding proteins, even the native

a


```
                    KTI motif                                    [F/Y]DPLGL motif
BoWSCP    MKTFFLVTLLLAAAVCTHGREQVKDSNGNPVKRGAKYFIQPAKSNGGGLVPAAINILPFCPLGITQTLLPYQP  73
WSCP-His  ----------------MAREQVKDSNGNPVKRGAKYFIQPAKSNGGGLVPAAINILPFCPLGITQTLLPYQP  56

BoWSCP    GLPVSFGYEPVIVGTDYIYTSTTINIEFRSEIWPVCNELSKLWAVDVSSSAAKEPAIIIGGESTAPNSLFKIE  146
WSCP-His  GLPVSFGYEPVIVGTDYIYTSTTINIEFRSEIWPVCNELSKLWAVDVSSSAAKEPAIIIGGESTAPNSLFKIE  129

BoWSCP    EATGAHTYKLTTSSGTVGTIPGPWLGAPQLIATNDEAKTLFVKFVKVDDDATKATTSTSRVEKLGLRMFPFY   218
WSCP-His  EATGAHTYKLTTSSGTVGTIPGPWLGAPQLIATNDEAKTLFVKFVKVDDDARSHHHHHHHHHH---------   192
```

b **c** **d**

e **f**

Figure 3. Purification of pigment-bound WSCP-His produced in Chl *a* synthesizing *Rba. sphaeroides*. (a) Sequence alignment of apo BoWSCP and recombinant WSCP-His used in this study. Positions of the Kunitz trypsin inhibitor (KTI) and [F/Y]DPLGL chlorophyll binding motifs are indicated by black bars. The 19 residue N-terminal endoplasmic reticulum signal peptide (underlined) and 21 residue C-terminal extension peptide (gray box) that are post-translationally cleaved in holo BoWSCP are absent in WSCP-His, which has a 10xHis-tag (shown in bold). (b) Photograph of purified WSCP-His. (c) SDS-PAGE and anti-6-His immunoblot analysis of purified WSCP-His. Lanes 1 and 2 contain 20 μg and 5 μg of protein, respectively. Lane M = Precision Plus Protein Standards (Biorad). (d) Absorption (Abs, solid green line) and fluorescence (Flu, dotted blue line) spectra of pigment bound WSCP-His. (e) Mass spectrum showing [M + H]$^+$ ions for GG-Chl *a* and DHGG-Chl *a*. Also detectable are the mono- and dioxidation products of GG-Chl *a*, DHGG-Chl *a* and THGG-Chl *a* formed by exposure to air during isolation and storage. Mass assignments were obtained at an accuracy of <3 ppm with external calibration and identifications were confirmed by isotope pattern (see Figure S2). (f) Mass spectrum showing the expected positions of [M + H]$^+$ ions for Chlide *a* and its mono-oxidation product, neither of which are detected.

Table 1. Absorption Peaks (nm) of Purified WSCP-His in 200 mM Tris-HCl (pH 8.0) at 25 °C

Protein	Soret				Q	
WSCP-His expressed in *Rba. sphaeroides* ΔCXFGP::*chlGP* WSCP^{+a}	342	384	418	436	628	673
Native BoWSCP[b]	343	384	423	437	629	673
BoWSCP-His expressed in *E. coli* (thylakoid membrane reconstituted)[b]	342	383	422	437	629	673
BoWSCP-His expressed in *E. coli* (Chl *a* reconstituted)[b,c]	342/343	384	417/421	436/437	629/630	673/674

[a]This study. [b]Ref 14. [c]Ref 17.

BChl pathway shuts down, no doubt to avoid the production of potentially phototoxic pigments. Further optimization of the introduced Chl pathway can now be attempted by altering the native photosynthetic apparatus to incorporate Chl *a* or introducing foreign Chl *a*-utilizing photosystem apoproteins. These ambitious aims require heterologous expression of multiple membrane proteins and further engineering of both pigment biosynthesis and assembly pathways.

■ METHODS

Growth Conditions. *Rba. sphaeroides* strains were grown microoxically in the dark in a rotary shaker (150 rpm) at 34 °C

in liquid M22+ medium[19] supplemented with 0.1% casamino acids.

Escherichia coli strains JM109[20] and S17−1[21] with pK18mobsacB or pIND4 plasmids were grown shaking (250 rpm) at 37 °C in LB medium supplemented with 30 μg·ml^{-1} kanamycin. For strains and plasmids used in this study see Table S3.

Construction of Mutants of *Rba. sphaeroides*. The *Rba. sphaeroides bchG* and *bchP* genes were replaced with their counterparts from *Synechocystis* (*chlG* and *chlP*, respectively) using the allelic exchange vector pK18mobsacB.[22] Briefly, the *chl* genes were codon-optimized for expression in *Rba. sphaeroides* using J-Cat,[23] and these sequences, flanked by the up- and downstream regions of the target for replacement, were synthesized by Bio Basic (Ontario, Canada). The fragments were subcloned into pK18mobsacB cut with *Eco*RI/*Hin*dIII. Sequenced clones were conjugated into *Rba. sphaeroides* from *E. coli* S17−1, and transconjugants in which the clone had integrated into the genome by homologous recombination were selected on M22+ medium supplemented with 30 μg· ml^{-1} kanamycin. Transconjugants that had undergone a second recombination were subsequently selected on M22+ supplemented with 10% (w/v) sucrose and lacking kanamycin. Sucrose-resistant, kanamycin-sensitive colonies had excised the allelic exchange vector through the second recombination event.[24] Gene replacements were confirmed by sequencing at the relevant loci. Sequences of primers used in this study can be found in Table S4.

Strains harboring the gene encoding BoWSCP were created as follows. The gene (designed and synthesized as above) encoding C-terminally 10xHis-tagged holo-BoWSCP, flanked by *Nco*I and *Hin*dIII restriction sites, was codon-optimized for expression in *Rba. sphaeroides*. The fragment was digested and cloned into the *Nco*I/*Hin*dIII sites of pIND4.[25] The resulting sequenced plasmid was conjugated into relevant strains of *Rba. sphaeroides* from *E. coli* S17−1 and transconjugants were selected for and maintained on M22+ medium supplemented with 30 μg·ml^{-1} kanamycin.

Pigment Analysis. Pigments were extracted from cell pellets after washing in 20 mM HEPES pH 7.2 by adding 9 pellet volumes of 0.2% (v/v) ammonia in methanol, vortex-mixing for 30 s and incubating on ice for 20 min. The extracts were clarified by centrifugation (15000 *g* for 5 min at 4 °C) and the supernatants were immediately analyzed on an Agilent 1200 HPLC system. (B)Chl *a* species were separated on a Phenomenex Aqua C18 reverse-phase column (5 μm particle size, 125 Å pore size, 250 mm × 4.6 mm) using a method modified from that of Addlesee and Hunter.[26] Solvents A and B were 64:16:20 (v/v) methanol/acetone/H$_2$O and 80:20 (v/v) methanol/acetone, respectively. The buffer composition changed from 0 to 100% solvent B over 10 min, and was maintained at 100% for 15 min, during which time (B)Chl species were eluted. Elution of Chl *a* species were monitored by checking absorbance at 665 nm or fluorescence emission at 670 nm with excitation at 431 nm, while elution of BChl *a* species were monitored by checking absorbance at 770 nm. To compare how much Chl *a* is produced in engineered strains compared to BChl *a* in the wildtype, the areas of HPLC peaks (detected by absorbance at 665 nm for Chl *a* species or 770 nm for BChl *a*) were integrated and the molar stoichiometry estimated using literature reported extinction coefficients for Chl *a*[27] and BChl *a*.[28]

Pigment from ∼500 μg of WSCP-His in 200 μL IMAC elution buffer (see below) was extracted as above and isolated by solid phase extraction as previously described.[29] The sample was dried under nitrogen, dissolved in 20 μL methanol and infused at 3 μL·min^{-1} via an atmospheric pressure chemical ionization source into a Maxis UHR-TOF mass spectrometer (Bruker Daltonics) operating with the following parameters: capillary potential: 4 kV, corona current: 4 μA, dry gas: 3.5 L· min^{-1} at 220 °C, nebulizer gas: 2 bar, vaporiser temperature 350 °C, ion cooler transfer time: 60 μs. All other parameters were as per the manufacturer's default settings.

Purification of WSCP-His from *Rba. sphaeroides* and Identification by Nanoflow LC−MS/MS. Expression of WSCP-His from pIND4 was induced in *Rba. sphaeroides* cultures at OD$_{710}$ 0.8 by addition of isopropyl β-D-1-thiogalactopyranoside (IPTG) to a final concentration of 125 μM. Cultures were harvested by centrifugation (6300 *g* for 15 min at 4 °C) 12 h after induction. Cell pellets were resuspended in binding buffer (25 mM HEPES pH 7.5, 500 mM NaCl, 5 mM imidazole) and broken by sonication on ice (6 × 30 s bursts separated by 30 s gaps). The clarified cell-free extract was isolated as the supernatant following centrifugation (43000 *g* for 20 min at 4 °C), passed through a 0.4 μm filter and fractionated by immobilized Ni-affinity chromatography. Following sequential washes with at least 10 column volumes of binding buffer containing 5, 20, 50, and 100 mM imidazole, remaining bound protein was eluted with 400 mM imidazole in 25 mM HEPES pH 7.5 with 100 mM NaCl. Protein fractions were analyzed by SDS polyacrylamide gel electro-phoresis and stained with Coomassie Brilliant Blue, or transferred onto a polyvinylidene fluoride membrane for immunodetection. Membranes were incubated with an anti-6-His primary antibody (Bethyl) followed by a secondary antibody conjugated with horseradish peroxidase (Sigma-Aldrich).

To identify WSCP-His by nanoflow LC−MS/MS, 50 μg protein (3 μL) was diluted to 10 μL with 100 mM Tris-HCl pH 8.5 containing 8 M urea and 5 mM DTT and incubated at 37 °C for 30 min. S-alkylation was carried out by addition of 1 μL 100 mM iodoacetic acid followed by incubation in the dark at room temperature for 30 min. Two μg trypsin/ endoproteinase LysC mix (Promega) was added and the protein digested at 37 °C for 3 h. After dilution with 75 μL 50 mM Tris-HCl pH 8.5, 10 mM CaCl$_2$, digestion was continued overnight. The digest was desalted using a C$_{18}$ spin column (Thermo Scientific) following the manufacturer's instructions and 500 ng analyzed by nanoflow liquid chromatography (Dionex UltiMate 3000 RSLCnano system) coupled online to a Q Exactive HF mass spectrometer (Thermo Scientific). Mass spectra were processed using Mascot Distiller v. 2.5.1.0 for database searching with Mascot Server v. 2.5.1 (Matrix Science) against NCBInr (Viridiplantae).

■ ASSOCIATED CONTENT

Ⓢ Supporting Information

The Supporting Information is available free of charge on the ACS Publications website at DOI: 10.1021/acssynbio.6b00069.

> Growth of *Synechocystis* and construction of a Δ*chlP* mutant; Figure S1: Construction of a *chlP* (sll1091) mutant in *Synechocystis* sp. PCC6803; Figure S2: Observed and theoretical isotopic patterns for mono-oxidized geranylgeranyl-chlorophyll *a*; Table S1: Nucleo-

tide sequences of codon optimized genes used in this study; Table S2: Identification of WSCP-His by nanoflow LC−MS/MS; Table S3: Strains and plasmids described in this study; Table S4: Primers used in this study. (PDF)

■ AUTHOR INFORMATION

Corresponding Author
*E-mail: c.n.hunter@sheffield.ac.uk.

Present Address
§Department of Biochemistry and Molecular Biology, The Pennsylvania State University, Pennsylvania 16802, United States.

Author Contributions
C.N.H. and D.P.C. conceived the study. A.H., P.J.J., J.W.C. and D.P.C performed the experiments. All authors designed the experiments and analyzed and interpreted the data. A.H., P.J.J., J.W.C., C.N.H. and D.P.C. wrote the manuscript.

Notes
The authors declare no competing financial interest.

■ ABBREVIATIONS

(B)Chl, (bacterio)chlorophyll; *Rba*, *Rhodobacter*; Chlide, Chlorophllide *a*; IMAC, immobilized metal affinity chromatography; LH, light harvesting complex; RC, reaction center; WSCP, water-soluble chlorophyll protein; GG, geranylgeranyl; DHGG, dihydrogeranylgeranyl; THGG, tetrahydrogeranylgeranyl.

■ REFERENCES

(1) Blankenship, R. E., Tiede, D. M., Barber, J., Brudvig, G. W., Fleming, G., Ghirardi, M., Gunner, M. R., Junge, W., Kramer, D. M., Melis, A., Moore, T. A., Moser, C. C., Nocera, D. G., Nozik, A. J., Ort, D. R., Parson, W. W., Prince, R. C., and Sayre, R. T. (2011) Comparing photosynthetic and photovoltaic efficiencies and recognizing the potential for improvement. *Science* 332, 805−809.
(2) Ort, D. R., Merchant, S. S., Alric, J., Barkan, A., Blankenship, R. E., Bock, R., Croce, R., Hanson, M. R., Hibberd, J. M., Long, S. P., Moore, T. A., Moroney, J., Niyogi, K. K., Parry, M. A., Peralta-Yahya, P. P., Prince, R. C., Redding, K. E., Spalding, M. H., van Wijk, K. J., Vermaas, W. F., von Caemmerer, S., Weber, A. P., Yeates, T. O., Yuan, J. S., and Zhu, X. G. (2015) Redesigning photosynthesis to sustainably meet global food and bioenergy demand. *Proc. Natl. Acad. Sci. U. S. A.* 112, 8529−8536.
(3) Hanna, M. C., and Nozik, A. J. (2006) Solar conversion efficiency of photovoltaic and photoelectrolysis cells with carrier multiplication absorbers. *J. Appl. Phys.* 100, 074510.
(4) Gomez Maqueo Chew, A., and Bryant, D. A. (2007) Chlorophyll biosynthesis in bacteria: the origins of structural and functional diversity. *Annu. Rev. Microbiol.* 61, 113−129.
(5) Partensky, F., Hess, W. R., and Vaulot, D. (1999) *Prochlorococcus*, a marine photosynthetic prokaryote of global significance. *Microbiol. Mol. Biol. Rev.* 63, 106−127.

(6) Sener, M., Strümpfer, J., Timney, J. A., Freiberg, A., Hunter, C. N., and Schulten, K. (2010) Photosynthetic vesicle architecture and constraints on efficient energy harvesting. *Biophys. J.* 99, 67−75.
(7) Cartron, M. L., Olsen, J. D., Sener, M., Jackson, P. J., Brindley, A. A., Qian, P., Dickman, M. J., Leggett, G. J., Schulten, K., and Hunter, C. N. (2014) Integration of energy and electron transfer processes in the photosynthetic membrane of *Rhodobacter sphaeroides*. *Biochim. Biophys. Acta, Bioenerg.* 1837, 1769−1780.
(8) Canniffe, D. P., and Hunter, C. N. (2014) Engineered biosynthesis of bacteriochlorophyll *b* in *Rhodobacter sphaeroides*. *Biochim. Biophys. Acta, Bioenerg.* 1837, 1611−1616.
(9) Chi, S. C., Mothersole, D. J., Dilbeck, P., Niedzwiedzki, D. M., Zhang, H., Qian, P., Vasilev, C., Grayson, K. J., Jackson, P. J., Martin, E. C., Li, Y., Holten, D., and Hunter, C. N. (2015) Assembly of functional photosystem complexes in *Rhodobacter sphaeroides* incorporating carotenoids from the spirilloxanthin pathway. *Biochim. Biophys. Acta, Bioenerg.* 1847, 189−201.
(10) Satoh, H., Uchida, A., Nakayame, K., and Okada, M. (2001) Water-soluble chlorophyll protein in *Brassicaceae* plants is a stress-induced chlorophyll-binding protein. *Plant Cell Physiol.* 42, 906−911.
(11) Canniffe, D. P., Chidgey, J. W., and Hunter, C. N. (2014) Elucidation of the preferred routes of C8-vinyl reduction in chlorophyll and bacteriochlorophyll biosynthesis. *Biochem. J.* 462, 433−440.
(12) Kim, E. J., and Lee, J. K. (2010) Competitive inhibitions of the chlorophyll synthase of *Synechocystis* sp. strain PCC 6803 by bacteriochlorophyllide *a* and the bacteriochlorophyll synthase of *Rhodobacter sphaeroides* by chlorophyllide a. *J. Bacteriol.* 192, 198−207.
(13) Addlesee, H. A., Gibson, L. C., Jensen, P. E., and Hunter, C. N. (1996) Cloning, sequencing and functional assignment of the chlorophyll biosynthesis gene, *chlP*, of *Synechocystis* sp. PCC 6803. *FEBS Lett.* 389, 126−130.
(14) Takahashi, S., Yanai, H., Nakamaru, Y., Uchida, A., Nakayama, K., and Satoh, H. (2012) Molecular cloning, characterization and analysis of the intracellular localization of a water-soluble Chl-binding protein from Brussels sprouts (*Brassica oleracea var. gemmifera*). *Plant Cell Physiol.* 53, 879−891.
(15) Takahashi, S., Uchida, A., Nakayama, K., and Satoh, H. (2014) The C-terminal extension peptide of non-photoconvertible water-soluble chlorophyll-binding proteins (Class II WSCPs) affects their solubility and stability: comparative analyses of the biochemical and chlorophyll-binding properties of recombinant *Brassica*, *Raphanus* and *Lepidium* WSCPs with or without their C-terminal extension peptides. *Protein J.* 33, 75−84.
(16) Vizcaíno, J. A., Deutsch, E. W., Wang, R., Csordas, A., Reisinger, F., Ríos, D., Dianes, J. A., Sun, Z., Farrah, T., Bandeira, N., Binz, P. A., Xenarios, I., Eisenacher, M., Mayer, G., Gatto, L., Campos, A., Chalkley, R. J., Kraus, H. J., Albar, J. P., Martinez-Bartolomé, S., Apweiler, R., Omenn, G. S., Martens, L., Jones, A. R., and Hermjakob, H. (2014) ProteomeXchange provides globally co-ordinated proteomics data submission and dissemination. *Nat. Biotechnol.* 30, 223−226.
(17) Takahashi, S., Ono, M., Uchida, A., Nakayama, K., and Satoh, H. (2013) Molecular cloning and functional expression of a water-soluble chlorophyll-binding protein from Japanese wild radish. *J. Plant Physiol.* 170, 406−412.
(18) Jones, M. R., Fowler, G. J. S., Gibson, L. C. D., Grief, G. G., Olsen, J. D., Crielaard, W., and Hunter, C. N. (1992) Mutants of *Rhodobacter sphaeroides* lacking one or more pigment-protein complexes and complementation with reaction centre, LH1, and LH2 genes. *Mol. Microbiol.* 6, 1173−84.
(19) Hunter, C. N., and Turner, G. (1988) Transfer of genes coding for apoproteins of reaction centre and light-harvesting LH1 complexes to *Rhodobacter sphaeroides*. *Microbiology* 134, 1471−1480.
(20) Yanisch-Perron, C., Vieira, J., and Messing, J. (1985) Improved M13 phage cloning vectors and host strains: nucleotide sequences of the M13mpl8 and pUC19 vectors. *Gene* 33, 103−119.

(21) Simon, R., Priefer, U., and Pühler, A. (1983) A broad host range mobilization system for *in vivo* genetic engineering: transposon mutagenesis in Gram negative bacteria. *Bio/Technology 1*, 784−791.

(22) Schäfer, A., Tauch, A., Jäger, W., Kalinowski, J., Thierbach, G., and Pühler, A. (1994) Small mobilizable multi-purpose cloning vectors derived from the *Escherichia coli* plasmids pK18 and pK19: selection of defined deletions in the chromosome of *Corynebacterium glutamicum. Gene 145*, 69−73.

(23) Grote, A., Hiller, K., Scheer, M., Münch, R., Nörtemann, B., Hempel, D. C., and Jahn, D. (2005) JCat: a novel tool to adapt codon usage of a target gene to its potential expression host. *Nucleic Acids Res. 33*, W526−W531.

(24) Hamblin, P. A., Bourne, N. A., and Armitage, J. P. (1997) Characterization of the chemotaxis protein CheW from *Rhodobacter sphaeroides* and its effect on the behaviour of *Escherichia coli. Mol. Microbiol. 24*, 41−51.

(25) Ind, A. C., Porter, S. L., Brown, M. T., Byles, E. D., de Beyer, J. A., Godfrey, S. A., and Armitage, J. P. (2009) Inducible-expression plasmid for *Rhodobacter sphaeroides* and *Paracoccus denitrificans. Appl. Environ. Microbiol. 75*, 6613−6615.

(26) Addlesee, H. A., and Hunter, C. N. (1999) Physical mapping and functional assignment of the geranylgeranyl-bacteriochlorophyll reductase gene, *bchP*, of *Rhodobacter sphaeroides. J. Bacteriol. 181*, 7248−7255.

(27) Porra, R. K., Thompson, W. A., and Kriedemann, P. E. (1989) Determination of accurate extinction coefficients and simultaneous equations for assaying chlorophylls a and b extracted with four different solvents:verification of the concentration of chlorophyll standardsby atomic absorption spectroscopy. *Biochim. Biophys. Acta, Bioenerg. 975*, 384−94.

(28) Permentier, H. P., Schmidt, K. A., Kobayashi, M., Akiyama, M., Hager-Braun, C., Neerken, S., Miller, M., and Amesz, J. (2000) Composition and optical properties of reaction centre core complexes from the green sulfur bacteria *Prosthecochloris aestuarii* and *Chlorobium tepidum. Phtosynth. Res. 64*, 27−39.

(29) Canniffe, D. P., Jackson, P. J., Hollingshead, S., Dickman, M. J., and Hunter, C. N. (2013) Identification of an 8-vinyl reductase involved in bacteriochlorophyll biosynthesis in *Rhodobacter sphaeroides* and evidence for the existence of a third distinct class of the enzyme. *Biochem. J. 450*, 397−405.